Removal and Separation of Hg(II) Ions from Aqueous Solutions by Macroporous Polystyrene-co-Divinylbenzene-Supported Polyamine Chelating Resins

Rongjun Qu,*,† Jianhui Liu,‡ Changmei Sun,† Ying Zhang,† Chunnuan Ji,† and Ping Yin†

School of Chemistry and Materials Science, Ludong University, Yantai 264025, China, and Monitoring and Analyzing Laboratory, Yantai Environmental Monitoring Centre, Yantai 264025, China

Three polyamine-functionalized macroporous polystyrene-co-divinylbenzene beads prepared by ethylenediamine (EDA), diethylenetriamine (DETA), and triethylenetetramine (TETA) modification, respectively (called PS-EDA, PS-DETA, and PS-TETA), have been investigated as high-capacity chelating resins for Hg(II) ions. Their structures were characterized by elemental analysis, infrared spectroscopy, and porous analysis. PS-EDA, PS-DETA, and PS-TETA were found to be highly effective for the adsorption of Hg(II) ions, exhibiting uptake capacities of (1.55, 1.73, and 1.84) mmol of Hg(II) ions/g of adsorbent, respectively. Kinetic data indicated that the adsorption process achieved equilibrium within 10 h and followed a pseudo-second-order rate equation. The adsorption isotherm data fit the Frendlich model and its linearized form well, together with thermodynamic data indicating the spontaneous and endothermic nature of the process. Results of a desorption study showed that Hg(II) ions adsorbed onto PS-EDA, PS-DETA, and PS-TETA could be easily desorbed. PS-EDA, PS-DETA, and PS-TETA show excellent affinity for Hg(II) ions, removing them from mixed metal solutions at pH 2.0. The highest effectiveness of PS-TETA for the capture of Hg(II) ions is attributed to both the longer polyamine chain and the expansion capability of the polystyrene-co-divinylbenzene framework, which facilitates the accessibility of the binding sites.

1. Introduction

Water pollution due to toxic metals in industry wastewaters has become a major issue worldwide. Investigations have shown that exposure to Hg(II) ions can have toxic effects on reproduction, the central nervous system, liver, and kidneys and cause sensory and psychological impairments. It is estimated that approximately two-thirds of Hg(II) ions in natural environments are of anthropogenic origin.[1] Hg(II) ions are mainly generated by sources such as electrical, paints, chlor-alkali, and the pharmaceutical, pulp, oil refining, plastic, and battery manufacturing industries.

Many techniques including precipitation, ion exchange, and adsorption are available to minimize the adverse effects of Hg(II) ions in the environment. Adsorption as a wastewater treatment process has been found to be an economically feasible alternative for Hg(II) ion removal.[2,3] Several materials such as activated carbon,[4,5] chelating resins,[6–8] chitosan,[9] clays,[10] and functionalized silica[3,11] have been studied for removal of Hg(II) ions from aqueous solutions.

In the above-mentioned adsorbents, only a limited number of them have been utilized on the adsorption of Hg(II) in multicomponent solutions. Generally, Hg(II) exists in multicomponent solutions in the industrial wastewaters. It is well-known that chelating resins with complex ligands containing nitrogen have excellent adsorption selectivity for divalent transition metal cations such as Hg(II) due to the strong affinity between the nitrogen atom and these metal ions. Many studies have demonstrated that adsorption materials containing functional groups of polyamine, which contain several nitrogen atoms in their molecular structures, exhibit good adsorption properties, and adsorption selectivity for Hg(II).[12–15]

In this study, three kinds of chelating resins of macroporous polystyrene-co-divinylbenzene beads modified, respectively, with ethylenediamine (EDA), diethylenetriamine (DETA), and triethylenetetramine (TETA) were synthesized. The adsorption properties, desorption properties of the three resins for Hg(II), and the selectivity in a bi-ionic system were also investigated. Considering that processes of ore mining and smelting (in particular Zn and Cu smelting) are one of main sources of mercury emission to the environment and that wastewaters from mining and mineral processing are often characterized by low pH,[16] we select a lower pH 2.0 for adsorption investigation.

2. Experimental Section

2.1. Materials and Methods. Commercial macroporous chloromethylated polystyrene-co-divinylbenzene beads (chlorobeads, PS-Cl), degree of cross-linking 10 % DVB, chlorine content 19.85 %, were purchased from the Chemical Factory of Nankai University of China. Before use, PS-Cl was further purified by washing thoroughly to remove surface impurities using acetone and reflux-extraction in ethanol for 10 h. Ethylenediamine, diethylenetriamine, and triethylenetetramine, obtained from the Shanghai Chemical Factory of China, were both chemically pure and used as received. The organic solvents tetrahydrofuran (THF) and ethanol were redistilled just before use. The other reagents such as metal salts were analytical grade and used as received without any further purification. A concentration of 0.1 mol·L^{-1} Hg(II) stock solution was prepared by dissolving 3.4264 g of $Hg(NO_3)_2 \cdot H_2O$ in 100 mL of 0.6 % HNO_3. The working solutions with different concentrations of Hg(II) ions were prepared by appropriate dilutions of the stock solution immediately prior to their use. The initial pH of the solution

* Corresponding author. Tel.: +86 535 6699201. E-mail: rongjunqu@sohu.com or qurongjun@eyou.com.
† Ludong University.
‡ Yantai Environmental Monitoring Centre.

10.1021/je100246y
Published on Web 09/14/2010

Scheme 1. Synthesis Procedure for PS-EDA, PS-DETA, and PS-TETA

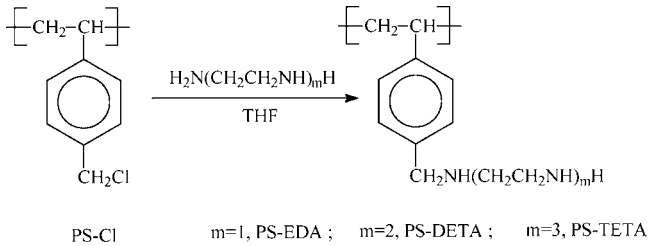

was adjusted to 2.0 with 0.01 mol·μL^{-1} HNO_3 and 0.01 mol·L^{-1} NaOH.

C and N analysis of products were subjected to elemental analysis by the Elementar VarioEL III instrument, Elementar Co., Germany. Infrared spectra were recorded on a Fourier transform infrared spectrophotometer, Nicolet MAGNA-IR 550 (series II) (Wisconsin, USA), using KBr pellets in the (4000 to 400) cm^{-1} region with a resolution of 4 cm^{-1}, by accumulating 32 scans. Porous structure parameters were characterized using an automatic physisorption analyzer ASAP 2020 by BET and BJH methods through N_2 adsorption at 77 K. Atomic absorption analysis of the various metal ions was performed with a flame atomic absorption spectrophotometer (model 932 GBH, Victoria Australia).

2.2. Synthesis of PS-EDA. The synthesis procedure was performed according to Scheme 1. First, 5.08 g (ca. 28.44 mmol Cl) of chloromethylated cross-linked polystyrene beads (PS-Cl) were suspended and swollen in 100 mL of tetrahydrofuran for 10 h. Then, 15 mL (ca. 224.12 mmol) of EDA was added, and the mixture solution was stirred for 1.5 h at room temperature (about 293 K) and refluxed for a further 24 h at 343 K under a nitrogen atmosphere. After cooling, the polymeric beads were filtered off and washed with distilled water and then 95 % ethanol. The product (PS-EDA) was transferred to a Soxhlet extraction apparatus for reflux-extraction in 95 % ethanol for 8 h and then was dried under vacuum at 323 K over 48 h.

2.3. Synthesis of PS-DETA. The reaction involved 5.08 g (ca. 28.44 mmol Cl) of PS-Cl, 100 mL of THF, and 24 mL (ca. 221.97 mmol) of DETA. The reaction conditions, time, and purification procedure of the product were similar to that of PS-EDA. The final product was denoted PS-DETA.

2.4. Synthesis of PS-TETA. The reaction involved 5.08 g (ca. 28.44 mmol Cl) of PS-Cl, 100 mL of THF, and 35 mL (ca. 234.98 mmol) of TETA. The reaction conditions, time, and purification procedure of the product were similar to that of PS-EDA. The final product was denoted PS-TETA.

2.5. Saturated Adsorption for Metal Ions. Static adsorption experiments were employed to determine the adsorption capabilities of PS-EDA, PS-DETA, and PS-TETA for different kinds of metal ions. In a thermostat-cum-shaking assembly, adsorption experiments were carried out by shaking 15.0 mg of chelating resins with 20 mL of an aqueous solution of metal ions of 5 mmol·L^{-1} in 50 mL Pyrex glass tubes at 298 K for 24 h at natural pH. Then the solutions in the tubes were separated from the resins, and the concentrations of metal ions were detected by means of atomic absorption spectrophotometry (AAS). The adsorption amounts were calculated according to eq 1

$$q = \frac{(C_0 - C)V}{W} \quad (1)$$

where q is the adsorption amount (mmol·g^{-1}), C_0 and C are the initial and the final concentrations of metal ions in solution, respectively (mmol·mL^{-1}), V is the volume of the solution (mL), and W is the weight of chelating resin (g).

2.6. Adsorption Kinetics. Adsorption kinetics were performed by mixing 15.0 mg of chelating resins with 20 mL of Hg(II) ions (5 mmol·L^{-1}, pH 2.0) solution in a 100 mL Erlenmeyer flask at different temperatures. One milliliter of the solution was taken at different time intervals, where the residual concentration of Hg(II) ions was determined via AAS.

2.7. Adsorption Isotherms. Complete adsorption isotherms were obtained by soaking 15.0 mg of chelating resins in a series of flasks containing 20 mL of different initial Hg(II) ions concentrations varying from (2.5 to 12.5) mmol·L^{-1} for 24 h. The initial pH was adjusted to 2.0 for Hg(II) ions while keeping the temperature at 298 K. Later on, the residual concentration was determined where the Hg(II) ion uptake was estimated via AAS.

2.8. Adsorption Selectivity of Hg(II) in Binary Ion Systems. The studies of the investigated resin toward Hg(II) in the presence of binary mixtures of Ni(II), Pb(II), Co(II), Cu(II), Zn(II), and Ag(I) was carried at room temperature (pH 2.0). The selectivity behavior of Hg(II) on the resins obtained was studied using static and dynamic methods. The estimation of these metal ions was also determined via AAS.

2.9. Desorption Studies. To investigate the desorption ability of adsorbed Hg(II) ions from the three resins, desorption experiments were carried out as follows: After adsorption, the Hg(II) ion-loaded resins were separated and slightly washed with distilled water to remove unadsorbed Hg(II) ion on the surface of the adsorbents. They were stirred with 20 mL of 0.5 mol·L^{-1} HNO_3 containing 5 % thiourea for 6 h, and the concentrations of Hg(II) ions were analyzed as previously. The desorption ratio of Hg(II) ions was then calculated as the ratio of the amount of desorbed Hg(II) ions to the amount of initially adsorbed Hg(II) ions.

3. Results and Discussion

3.1. Structural Characterization of the Chelating Resins. The structures of synthetic chelating resins PS-EDA, PS-DETA, and PS-TETA can be confirmed by comparing the IR spectra of PS-Cl before and after reaction with polyamines, as shown in Figure 1. The disappearance of the characteristic absorption peak of C−Cl at 676 cm^{-1}, and the appearance of new peaks at 3440 cm^{-1} and a broad peak at 1636 cm^{-1}, which are attributed to the stretching vibration and deformation vibration of N−H, respectively, after the reaction of PS-Cl with polyamine indicates that the functional groups EDA, DETA, and TETA were introduced successfully into the polymeric matrix.

Table 1 gives the N concentration of the chelating resins determined by elemental analysis. The elemental analysis results showed that the content of polyamine in the three kinds of chelating resins were (3.16, 2.28, and 1.82) mmol·g^{-1}, respectively, which are far less than their theoretical values (5.68, 4.57, and 3.82) mmol·g^{-1}, implying that the part of polyamine existed in the form of cross-linking in the resins. Obviously, the order of cross-linking degree is PS-TETA > PS-DETA > PS-EDA, which is in accordance with the order of the length of the chain of polyamine, meaning that the longer the chain of polyamine, the higher the cross-linking degree of polyamine. Table 1 also shows the porous structure parameters of the PS-Cl, PS-EDA, PS-DETA, and PS-TETA. As shown in Table 1, the values of BET surface area, and BJH desorption average pore diameter of pores for products, were greater than those of PS-Cl. This would suggest that new big pores were formed in the process

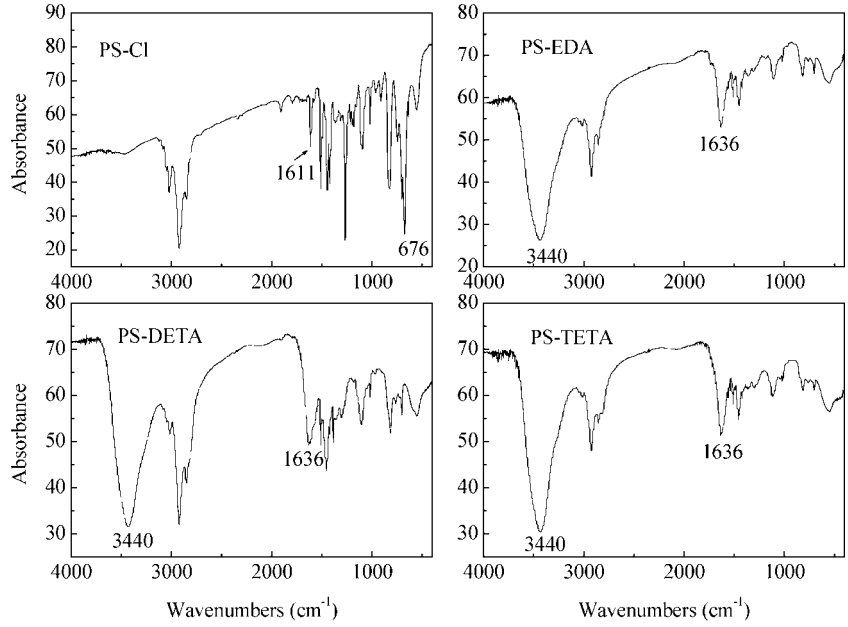

Figure 1. Infrared spectra of PS-Cl, PS-EDA, PS-DETA, and PS-TETA.

Table 1. Element Analysis and the Porous Structure Parameters of PS-Cl, PS-EDA, PS-DETA, and PS-TETA

				polyamine content (mmol·g^{-1})				
chelating resins	C (%)	H (%)	N (%)	observed	theoretical	BET surface area (m^2·g^{-1})	BJH desorption cumulative volume of pores (cm^3·g^{-1})[a]	BJH desorption average pore diameter (nm)
PS-Cl						31.85	0.31	36.66
PS-EDA	74.23	8.35	8.86	3.16	5.68	36.24	0.35	43.90
PS-DETA	68.91	8.40	9.56	2.28	4.57	35.00	0.39	42.64
PS-TETA	68.40	8.62	10.19	1.82	3.82	34.42	0.38	41.07

[a] The total volume of pores between 1.7 and 300 nm diameter.

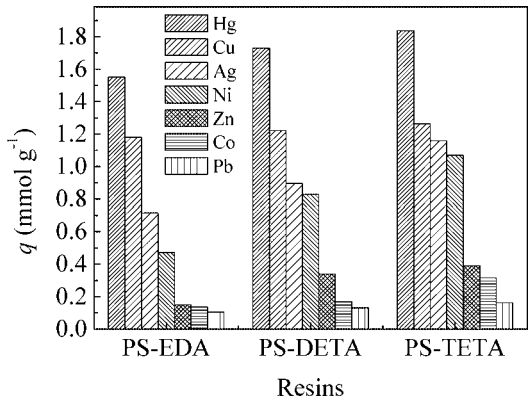

Figure 2. The saturated adsorption capacities of chelating resins for metal ions (298 K, pH = 2.0).

of synthesis because of intra- and interstrand cross-linking reaction of polyamine.[17] Another reason for this should not be ignored, that is, the introduction of strong polar groups [$NH_2(CH_2CH_2NH)$mH, m = 1,2,3]) into the weakly polar polystyrene matrix.[18]

3.2. Static Saturated Adsorption Capacities. In general, static saturated adsorption capacities under the natural pH conditions value were employed to initially evaluate the adsorption capabilities of metal ions. The static saturated adsorption capacities of PS-EDA, PS-DETA, and PS-TETA for Hg(II), Cu(II), Ag(I), Ni(II), Zn(II), Co(II), and Pb(II) are shown in Figure 2. From Figure 2, it can be observed that all three kinds of chelating resins exhibit better adsorption capacity for Hg(II) than for other metal ions, indicating that the three chelating resins may be used to selectively adsorb Hg(II) ions from complex systems. For the three kinds of chelating resins, the order of adsorption capacity for metal ions is as follows: PS-TETA > PS-DETA > PS-EDA. A possible explanation for this is that the higher content of functional groups (N%) gave rise to better coordination with Hg(II) ions. So the adsorption properties of Hg(II) was studied in detail.

3.3. Adsorption Kinetics. Kinetic studies provide an insight into the rate as well as mechanism of the adsorption process. The rate of adsorption on PS-EDA, PS-DETA, and PS-TETA was determined as a function of temperature. The uptake of Hg(II) ions over time at a pH of 2.0 for different temperatures [(278, 288, 298, and 308) K] of Hg(II) is shown in Figure 3. It is observed from Figure 3 that contact time significantly affects the mercury adsorption. The adsorption of PS-EDA, PS-DETA, and PS-TETA is very fast initially and then slowed considerably. The initial high rate is due to the abundance of free binding sites, which with time become saturated, resulting in a decreased adsorption rate. It was found that PS-EDA required at least 8 h to reach adsorption equilibrium, PS-DETA only 6 h, but PS-TETA 10 h. The fact may be interpreted as PS-TETA having a longer chain polyamine with more cross-linking structures which hinder the functional atoms coordinating with Hg(II) ions. For PS-DETA, the appropriate length of the polyamine chain with the better flexibility can enhance the adsorption rate. Hence, in the present study, we used 12 h as the contact time for further experiments to ensure complete adsorption. It is also very clear from the results that the maximum uptake of metal ions was slightly dependent on the temperature. It has been observed that the adsorption capacities of PS-EDA, PS-DETA, and PS-TETA

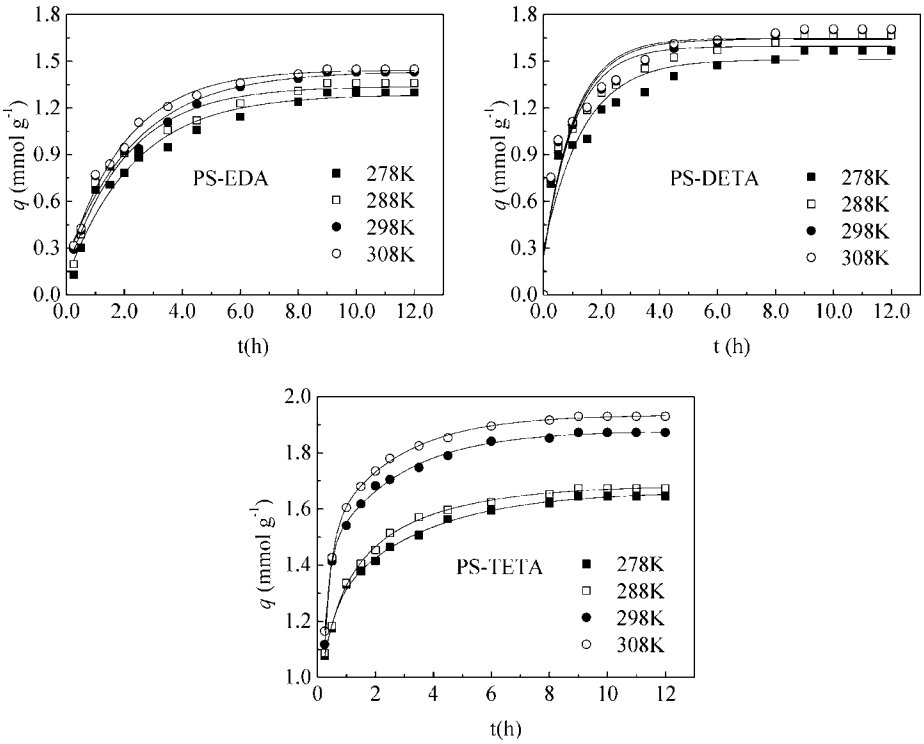

Figure 3. Adsorption kinetics of Hg(II) ions onto PS-EDA, PS-DETA, and PS-TETA. Adsorption conditions: initial concentration of Hg(II) ions, 5 mmol·L^{-1}; pH 2.0.

Table 2. Kinetic Parameters for the Adsorption of Hg(II) Ions onto PS-EDA, PS-DETA, and PS-TETA Resins at Various Temperatures

			pseudo-first-order kinetics			pseudo-second-order kinetics			
resins	T (K)	q_e(exp) (mmol·g^{-1})	k_1 (h^{-1})	q_e(cal) (mmol·g^{-1})	R_1^2	k_2 (g·$mmol^{-1}$·h^{-1})	q_e(cal) (mmol·g^{-1})	h_2 (mmol·g^{-1}·h^{-1})	R_2^2
PS-EDA	278	1.30	0.35	1.08	0.9806	0.33	1.54	0.78	0.9940
	288	1.36	0.37	1.08	0.9818	0.44	1.54	1.04	0.9982
	298	1.43	0.41	1.20	0.9905	0.45	1.61	1.17	0.9978
	308	1.45	0.45	1.19	0.9954	0.51	1.62	1.34	0.9989
PS-DETA	278	1.56	0.35	0.85	0.9909	0.83	1.66	2.29	0.9973
	288	1.66	0.39	0.87	0.9916	0.93	1.75	2.85	0.9992
	298	1.70	0.42	0.94	0.9932	0.93	1.79	2.98	0.9992
	308	1.71	0.45	0.94	0.9908	0.96	1.80	3.11	0.9992
PS-TETA	278	1.64	0.38	0.51	0.9905	1.95	1.69	5.57	0.9997
	288	1.67	0.43	0.53	0.9843	2.05	1.71	5.99	0.9998
	298	1.87	0.46	0.57	0.9704	2.07	1.91	7.55	0.9999
	308	1.93	0.48	0.60	0.9812	2.13	1.97	8.27	0.9999

for Hg(II) ions increase with increasing temperature in the range (278 to 308) K, indicating that the process of adsorption is endothermic. This was due to the increasing tendency of Hg(II) ions to adsorb from the solution to the interface as the temperature increased. In order to clarify the adsorption kinetics process of Hg(II) on PS-EDA, PS-DETA, and PS-TETA, two kinetic models, pseudo-first-order[19] and pseudo-second-order,[20] were applied to the experimental data.

The pseudo-first-order model is expressed as

$$\ln \frac{(q_e - q_t)}{q_e} = -k_1 t \qquad (2)$$

where k_1 is the pseudo-first-order rate constant (h^{-1}) of adsorption and q_e and q_t (mmol·g^{-1}) are the amounts of Hg(II) ions adsorbed at equilibrium and time t (h), respectively. The value of ln ($q_e - q_t$) is calculated from the experimental results and plotted against t (h). The experimental and calculated q_e values, pseudo-first-order rate constants, and regression coefficient (R_1^2) values are presented in Table 2.

As seen from Figure 4, the pseudo-first-order model fits the data well. The R_1^2 values were found to be in the range 0.9704−0.9954 for the adsorption of Hg(II) ions onto PS-EDA, PS-DETA, and PS-TETA. Although the plots show linearity, the calculated q_e values were not in agreement with the experimental q_e values, suggesting that the adsorption of Hg(II) does not follow pseudo-first-order kinetics. In order to find a more reliable description of the kinetics, a pseudo-second-order kinetic model was applied to the experimental data.

The pseudo-second-order model can be expressed as

$$\frac{t}{q_t} = \frac{1}{k_2 q_e^2} + \frac{t}{q_e} \qquad (3)$$

where k_2 is the pseudo-second-order rate of adsorption (g·$mmol^{-1}$·h^{-1}). The adsorption rate constant is one of the important kinetic parameters. The slope and intercept of the linear plot t/q_t vs t yielded the values of q_e and k_2. Additionally, the initial adsorption rate, h, has been widely used for evaluation of the adsorption rates. The initial adsorption rates (h, mmol·g^{-1}·h^{-1})

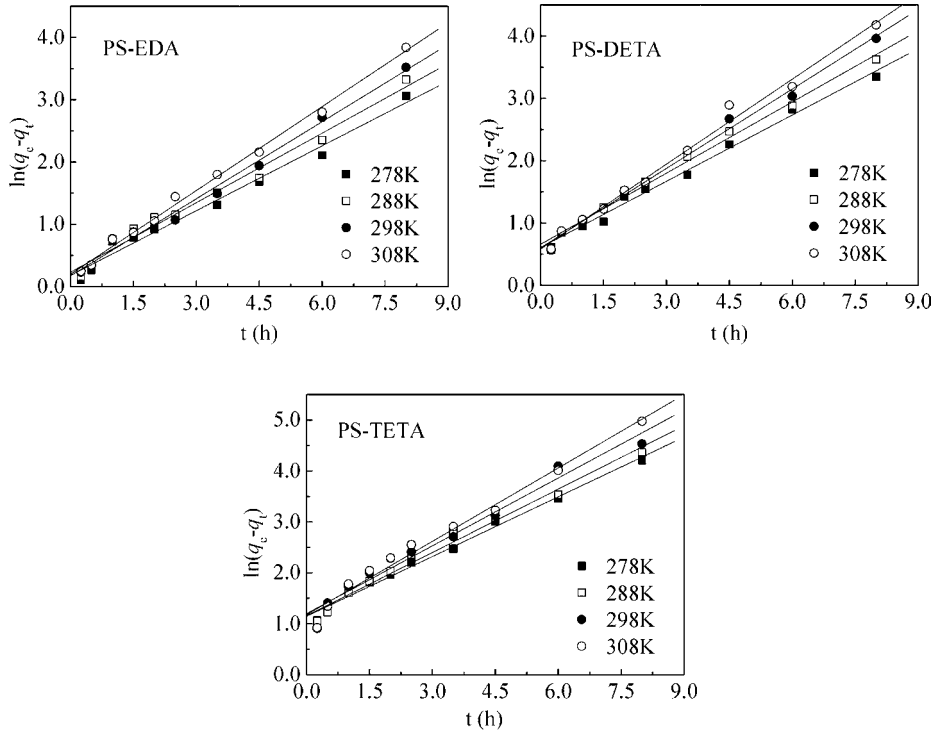

Figure 4. Pseudo-first-order kinetic plots for the adsorption of Hg(II) ions onto PS-EDA, PS-DETA, and PS-TETA.

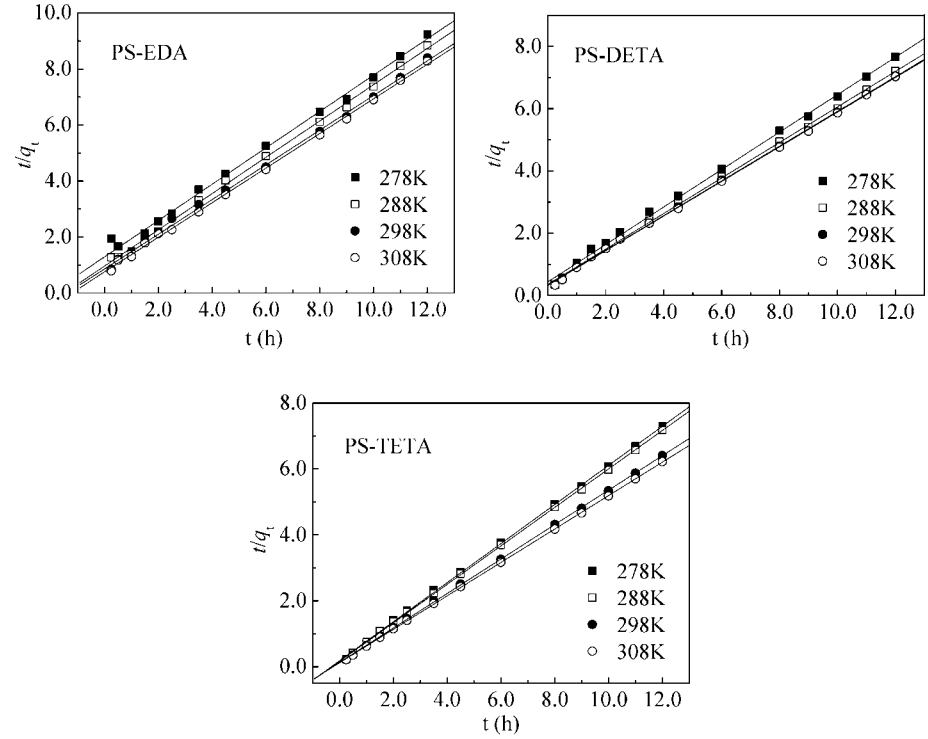

Figure 5. Pseudo-second-order kinetic plots for the adsorption of Hg(II) ions onto PS-EDA, PS-DETA, and PS-TETA.

of the PS-EDA, PS-DETA, and PS-TETA for Hg(II) ions can be determined from k_2 and q_e values using eq 4[21]

$$h = k_2 q_e^2 \tag{4}$$

The regression coefficients (R_2^2) and several parameters obtained from the pseudo-second-order kinetic model are also shown in Table 2. As seen from Figure 5 and Table 2, the pseudo-second-order model fits the data well and the obtained R_2^2 values are above 0.9940. Moreover, the calculated q_e values are in good agreement with experimental q_e values. Hence, the adsorption kinetics could well be approximated more favorably by a pseudo-second-order kinetic model for Hg(II) ions onto PS-EDA, PS-DETA, and PS-TETA. This is probably because the initial concentration of Hg(II) ions (C_0) that we selected is not too high.[22]

The values of k_2 for PS-EDA, PS-DETA, and PS-TETA increased with increasing temperature. Meanwhile, the initial adsorption rate increases with increasing temperature for the three

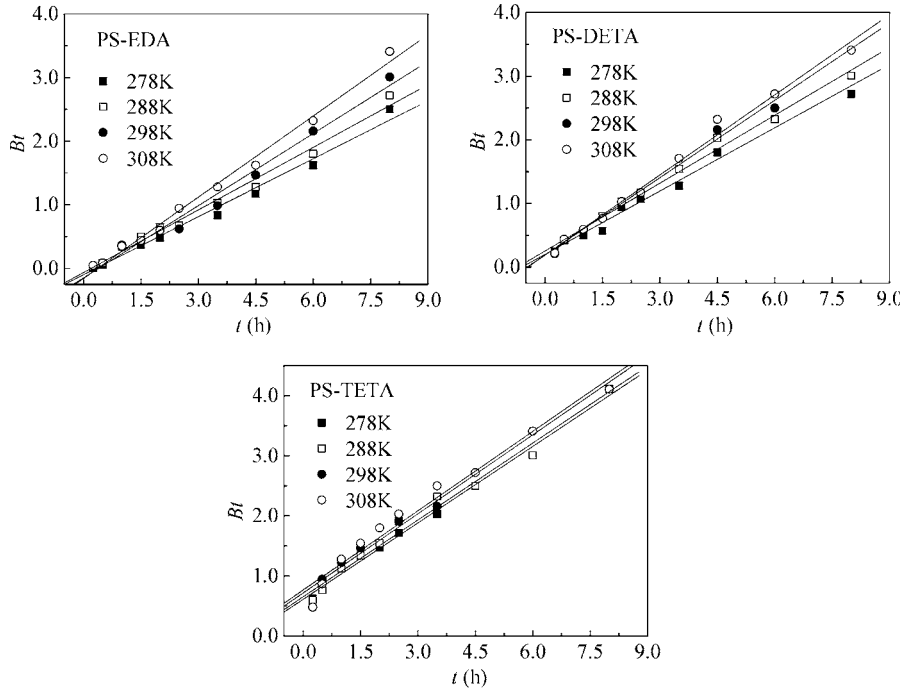

Figure 6. *Bt* vs time plots at different adsorbate temperatures of Hg(II) ions onto PS-EDA, PS-DETA, and PS-TETA.

resins. That might be because the diffusion rate of Hg(II) ions is enhanced by increasing temperature. For PS-EDA, PS-DETA, and PS-TETA, k_2 and h always increased with the length of the polyamine chain at any temperature. The above-mentioned fact demonstrated that the higher content of functional groups is more beneficial to increasing the adsorption rates for Hg(II) ions.

The kinetic data were further analyzed using the kinetic expression given by Boyd et al.[23] to check whether adsorption proceeds via an external diffusion or intraparticle diffusion mechanism, which is expressed as follows:

$$F = 1 - \frac{6}{\pi^2}\sum_{n=1}^{\infty}\frac{1}{n^2}\exp[-n^2Bt] \quad (5)$$

where n is an integer that defines the infinite series solution and F is the fractional attainment of equilibrium at time t and is obtained by the expression

$$F = \frac{q_t}{q_e} \quad (6)$$

where q_t is the amount of metal ions taken up at time t, and q_e is the amount of metal ion adsorbed at equilibrium and

$$B = \frac{\pi^2 D_i}{r_0^2} = \text{time constant} \quad (7)$$

where D_i is the effective diffusion coefficient of the ions in the adsorbent phase and r_0 is the radius of the adsorbent particle assumed to be spherical.

Values of *Bt* were obtained from corresponding values of *F*. *Bt* values for each *F* are given by Reichenberg,[24] and the results are plotted in Figure 6. The linear equations and coefficients of determination R^2 are given in Table 3.

Table 3. The *Bt* versus Time Linear Equations and Coefficients R^2

resins	T (K)	linear equation	R^2	intercept error
PS-EDA	278	$Bt = 0.3038t - 0.0999$	0.9845	0.0515
	288	$Bt = 0.3280t - 0.0652$	0.9875	0.0500
	298	$Bt = 0.3781t - 0.1484$	0.9853	0.0625
	308	$Bt = 0.4255t - 0.1569$	0.9921	0.0513
PS-DETA	278	$Bt = 0.3311t + 0.2021$	0.9871	0.0511
	288	$Bt = 0.3555t + 0.2535$	0.9910	0.0459
	298	$Bt = 0.4052t + 0.1907$	0.9938	0.0433
	308	$Bt = 0.4195t + 0.1898$	0.9908	0.0547
PS-TETA	278	$Bt = 0.4242t + 0.6104$	0.9925	0.0499
	288	$Bt = 0.4269t + 0.6512$	0.9852	0.0706
	298	$Bt = 0.4388t + 0.7172$	0.9813	0.0820
	308	$Bt = 0.4403t + 0.7641$	0.9730	0.0991

Linearity of this plot is employed to distinguish external-transport- (film diffusion) from intraparticle-transport-controlled rates of adsorption. A straight line passing through the origin is indicative of adsorption processes governed by particle-diffusion mechanisms; otherwise, they are governed by film diffusion.[25] In the present case, the plots were linear but without passing through the origin (Figure 6). This indicates that, for all resins, film diffusion is the rate-limiting adsorption process for Hg(II).

3.4. Thermodynamic Parameters of Adsorption. The activation energy (E_a) was obtained from the Arrhenius plot. The thermodynamic parameters obtained for the adsorption process were calculated by using the van't Hoff eq 9

$$\ln k_2 = \ln A - E_a/RT \quad (8)$$

$$\ln K_c = \frac{\Delta S^\circ}{R} - \frac{\Delta H^\circ}{RT} \quad (9)$$

where E_a is the Arrhenius activation energy, A is the Arrhenius factor, T is the absolute temperature (K), and R is the gas constant (8.314 J·mol^{-1}·K^{-1}). ΔS° (J·mol^{-1}·K^{-1}) and ΔH° (kJ·mol^{-1}) were calculated from the slope and intercept of linear plots of ln K_c vs $1/T$ for Hg(II) ions. The equilibrium constant

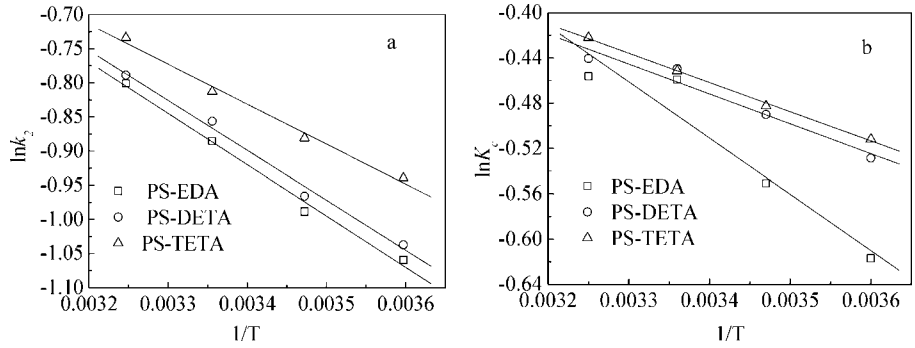

Figure 7. ln k_2 vs $1/T$ (a) and ln K_c vs $1/T$ plots for Hg(II) ions adsorption onto PS-EDA, PS-DETA, and PS-TETA.

Table 4. Thermodynamic Parameters of PS-EDA, PS-DETA, and PS-TETA for Hg(II) Ion Adsorption

resins	T (K)	$\Delta G°$ (kJ·mol^{-1})	$\Delta H°$ (kJ·mol^{-1})	$\Delta S°$ (J·K^{-1}·mol^{-1})	E_a (kJ·mol^{-1})
PS-EDA	278	−1.25	4.13	9.81	6.24
	288	−1.38			
	298	−1.56			
	308	−1.62			
PS-DETA	278	−1.36	2.19	3.49	6.08
	288	−1.46			
	298	−1.58			
	308	−1.65			
PS-TETA	278	−1.38	2.15	3.49	4.86
	288	−1.48			
	298	−1.58			
	308	−1.68			

(K_c) was calculated from the following relationship (eq 10).[26] The plot shown in Figure 7b is linear over the entire range of temperature investigated.

$$K_c = \frac{C_{Ae}}{C_e} \tag{10}$$

where C_{Ae} and C_e are the equilibrium concentrations of metal (mg·L^{-1}) on adsorbent and in solution, respectively.

The Gibbs energy change ($\Delta G°$) was calculated from the relation

$$\Delta G° = -RT \ln K_c \tag{11}$$

where T (K) is the absolute temperature, R (J·K^{-1}·mol^{-1}) is gas constant, and $\Delta G°$ is the standard Gibbs energy change.

From the slope of the linear plot of ln k_2 vs $1/T$ (shown in Figure 7a), the apparent activation energy was obtained as (6.24, 6.08, and 4.26) kJ·mol^{-1} for the adsorption of Hg(II) onto PS-EDA, PS-DETA, and PS-TETA, respectively. This low activation energy as compared to those of typical chemical reactions of (40 to 80) kJ·mol^{-1} implies that the adsorption of PS-EDA, PS-DETA, and PS-TETA for Hg(II) is a physisorption procedure.[27] The value of $\Delta G°$ for the adsorption of Hg(II) on PS-EDA, PS-DETA, and PS-TETA at different temperatures is given in Table 4. The magnitude of $\Delta G°$ increased with the rise in temperature. The negative value confirms the feasibility of the process and the spontaneous nature of adsorption of Hg(II) on PS-EDA, PS-DETA, and PS-TETA. The value of $\Delta H°$ was positive, indicating that the adsorption reaction is endothermic. This is also supported by the increase in value of uptake capacity of all the adsorbent with a rise in temperature up to 308 K. Enthalpy change data are also useful for distinguishing physisorption from the chemisorption. Physisorption is typically

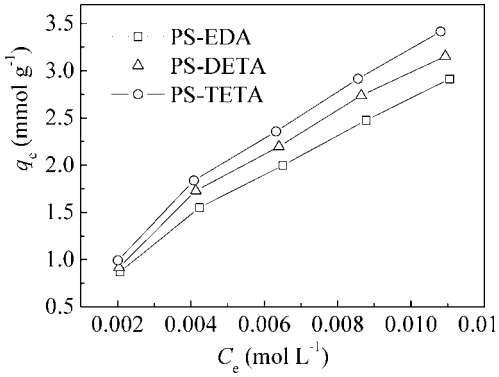

Figure 8. Isotherms for the adsorption of Hg(II) ions onto PS-EDA, PS-DETA, and PS-TETA at 298 K.

associated with heats of adsorption ranging from (2.1 to 20.9) kJ·mol^{-1}, while chemisorption corresponds to much larger $\Delta H°$ values of (20.9 to 418.4) kJ·mol^{-1}.[28] The enthalpy change result of PS-EDA (4.13 kJ·mol^{-1}), PS-DETA (2.19 kJ·mol^{-1}), and PS-TETA (2.15 kJ·mol^{-1}) is in the former range, which suggests that adsorption of Hg(II) on PS-EDA, PS-DETA, and PS-TETA is a physisorption process, which is consistent with the activation energy (E_a) obtained from the Arrhenius equation. The positive value of $\Delta S°$ reflects the affinity of Hg(II) for the resins used.[29,30] In addition, the positive value of $\Delta S°$ shows the increasing randomness at the solid/liquid interface during the adsorption of Hg(II) on the three resins.

3.5. Adsorption Isotherms. To investigate the adsorption capacity, a wide range of concentrations of Hg(II) solutions were shaken for 12 h with resins at 298 K. The adsorption isotherms for Hg(II) ions are presented in Figure 8.

The adsorption data usually follow either Langmuir or Freundlich isotherms.[31] The Langmuir isotherm is valid for monolayer adsorption onto a surface containing a finite number of identical sites. It can be mathematically represented as:

$$q_e = \frac{q_{the} K_L C_e}{1 + K_L C_e} \tag{12}$$

The linear expression of the Langmuir isotherm is eq 13:

$$\frac{C_e}{q_e} = \frac{C_e}{q_{the}} + \frac{1}{qK_L} \tag{13}$$

where q_e is the adsorption capacity (mmol·g^{-1}), C_e is the equilibrium concentration of metal ions (mmol·mL^{-1}), q_{the} is the theoretical saturation adsorption capacity (mmol·g^{-1}), and K_L is the Langmuir constant that is related to the affinity of binding sites

Table 5. Isotherm Parameters of the Langmuir Model and Freundlich Model for the Adsorption of Hg(II) Ions

	Langmuir				Freundlich		
adsorbents	q_{the} (mmol·g^{-1})	K_L (mL·mmol^{-1})	R_L^2	r_L	K_F (mmol·g^{-1})	1/n	R_F^2
PS-EDA	6.17	77.14	0.9811	0.051	72.69	0.71	0.9970
PS-DETA	6.86	76.74	0.9811	0.051	87.18	0.72	0.9907
PS-TETA	7.38	79.65	0.9833	0.050	92.75	0.72	0.9934

Table 6. The Static Adsorption Selectivity of PS-EDA, PS-DETA, and PS-TETA in Binary Ions Systems at 298 K (pH = 2.0)

resins	system	metal ions	adsorption capacity (mmol·g^{-1})	selective coefficient, α[a]
PS-EDA	Hg(II)-Ni(II)	Hg(II)	1.94	∞
		Pb(II)	0	
	Hg(II)-Pb(II)	Hg(II)	1.90	∞
		Ni(II)	0	
	Hg(II)-Co(II)	Hg(II)	1.89	∞
		Co(II)	0	
	Hg(II)-Cu(II)	Hg(II)	1.87	∞
		Cu(II)	0	
	Hg(II)-Ag(I)	Hg(II)	1.85	∞
		Ag(I)	0	
	Hg(II)-Zn(II)	Hg(II)	1.83	10.17
		Zn(II)	0.18	
PS-DETA	Hg(II)-Ni(II)	Hg(II)	2.16	∞
		Pb(II)	0	
	Hg(II)-Pb(II)	Hg(II)	2.03	∞
		Ni(II)	0	
	Hg(II)-Co(II)	Hg(II)	1.99	∞
		Co(II)	0	
	Hg(II)-Cu(II)	Hg(II)	1.95	∞
		Cu(II)	0	
	Hg(II)-Ag(I)	Hg(II)	1.94	∞
		Ag(I)	0	
	Hg(II)-Zn(II)	Hg(II)	1.92	7.68
		Zn(II)	0.25	
PS-TETA	Hg(II)-Ni(II)	Hg(II)	2.39	∞
		Pb(II)	0	
	Hg(II)-Pb(II)	Hg(II)	2.27	∞
		Ni(II)	0	
	Hg(II)-Co(II)	Hg(II)	2.38	∞
		Co(II)	0	
	Hg(II)-Cu(II)	Hg(II)	2.26	∞
		Cu(II)	0	
	Hg(II)-Ag(I)	Hg(II)	2.24	∞
		Ag(I)	0	
	Hg(II)-Zn(II)	Hg(II)	2.22	7.66
		Zn(II)	0.29	

[a] The selective coefficient is the ratio of adsorption capacities of metal ions in a binary mixture.

(mL·mmol^{-1}). By plotting C_e/q_e vs C_e, Langmuir's parameters q_{the} and K_L can be determined. Additionally, the important parameter, r_L, called the equilibrium parameter is calculated to identify whether an adsorption system is favorable or unfavorable.

$$r_L = \frac{1}{1 + K_L C_0} \tag{14}$$

where K_L (mL·mmol^{-1}) is the Langmuir constant and C_0 is the highest initial Hg(II) concentration (mmol·mL^{-1}). There are four probabilities for the r_L value: (i) for favorable adsorption, $0 < r_L < 1$; (ii) for unfavorable adsorption, $r_L > 1$; (iii) for linear adsorption, $r_L = 1$; (iv) for irreversible adsorption, $r_L = 0$. As seen from Table 5, the adsorption of Hg(II) ions on these three resins is favorable.[32]

The Freundlich model assumes heterogeneous adsorption due to the diversity of the adsorption sites or the diverse nature of the metal ion-adsorbed, free, or hydrolyzed species. The Freundlich model is expressed as:

$$q_e = K_F C_e^{1/n} \tag{15}$$

and the equation may be linearized by taking logarithms

$$\ln q_e = \ln K_F + \frac{\ln C_e}{n} \tag{16}$$

where q_e is the amount of solute adsorbed per unit weight of adsorbent (mmol·g^{-1}), C_e is the equilibrium concentration of solute in the bulk solution (mmol·L^{-1}), K_F is the binding energy constant reflecting the affinity of the adsorbents to metal ions, and n is the Freundlich exponent related to adsorption intensity.

The adsorption data fitted with both the Langmuir and Freundlich models is shown in Figure 9. Table 5 displays the coefficients of the Langmuir and Freundlich models along with regression coefficients (R^2). As seen from Table 5, the R^2 values for both the Langmuir and Freundlich isotherm models were above 0.98, suggesting that both models closely fit the experimental results. However, the R^2 values indicate that the Freundlich isotherm fits the experimental data slightly better than the Langmuir isotherm at room temperature. On average, a favorable adsorption tends to have Freundlich constant n between 1 and 10. A larger value of n (smaller value of 1/n) implies stronger interaction between adsorbent and heavy metal while 1/n equal to 1 indicates linear adsorption leading to identical adsorption energies for all sites.[33] The 1/n values for PS-EDA, PS-DETA, and PS-TETA were found to be 0.71, 0.72, and 0.72, respectively, suggesting that the adsorption of Hg(II)

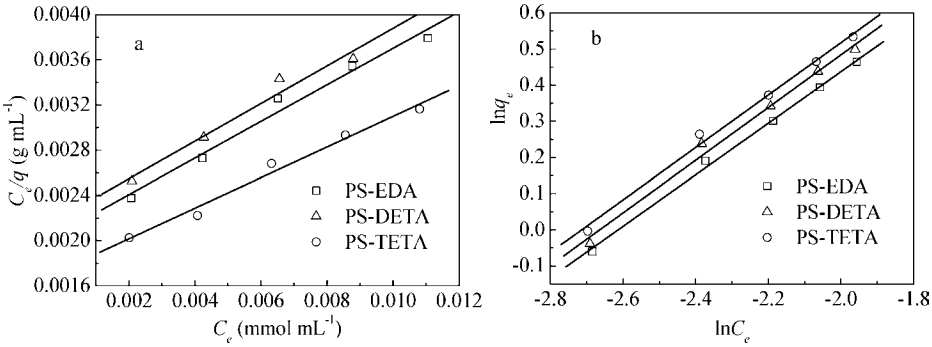

Figure 9. The Langmuir isotherms (a) and Freundlich isotherms (b) of PS-EDA, PS-DETA, and PS-TETA for Hg(II).

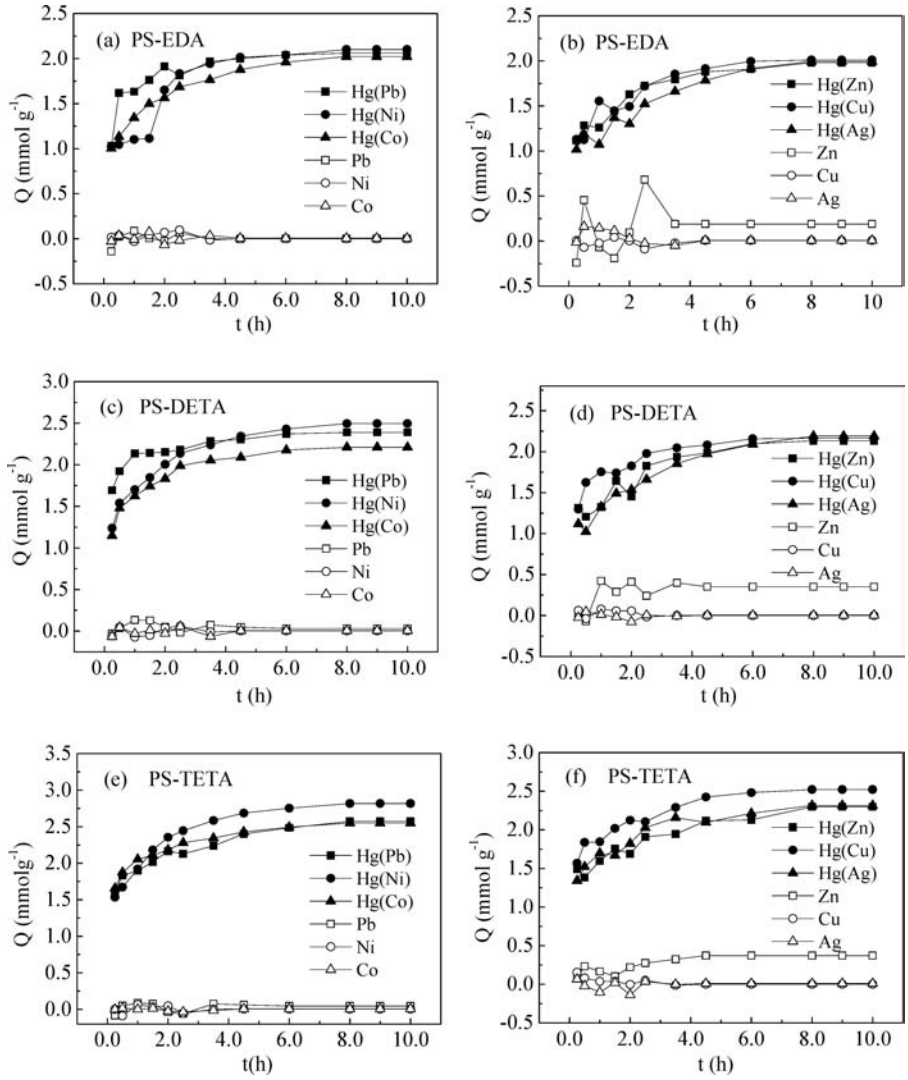

Figure 10. The dynamic adsorption selectivity of PS-EDA, PS-DETA, and PS-TETA in binary ions systems at 298 K (pH = 2.0).

on to PS-EDA, PS-DETA, and PS-TETA was favorable. The results are also coincident with the conclusions of the activation energy.

3.6. Selectivity Adsorption Studies. We further demonstrate the feasibility of designing highly selective resins based on macroporous polystyrene-co-divinylbenzene beads for the selective separation and recovery of Hg(II) from binary mixtures containing Ni(II), Pb(II), Co(II), Cu(II), Zn(II), and Ag(I) ions. The initial concentration of Hg(II) and coexisting ions were both 5 mmol·L^{-1} in binary mixtures for selective separation. The results using the static method are reported in Table 6 which show that the three resins exhibited good adsorption selectivity for Hg(II). This high adsorption selectivity was due to the high affinity of the Hg(II) ion for the polyamine group in polystyrene-co-divinylbenzene beads. According to the hard−soft acid−base (HSAB) theory, Hg(II) is classified as a soft ion. Soft ions form very strong bonds with groups containing nitrogen and sulfur atoms.[34] Therefore, PS-EDA, PS-DETA, and PS-TETA show a very high adsorption capacity for Hg(II) ions.[35]

Selective separation of Hg(II) using dynamic methods with other metal ions was also examined (see Figure 10) where similar results for that of individual metal ions were obtained. This implies that the studied resin could be used successfully in the selective separation of Hg(II) from the other investigated metal ions.

3.7. Desorption Studies. To investigate the feasibility of reusing the resins and Hg(II) ions, desorption experiments were conducted. The desorption was attempted by elution of the Hg(II)-loaded resins with 0.5 mol·L^{-1} HNO_3 containing 5 % thiourea. The desorption results of Hg(II)-loaded resins observed were 100 % for PS-EDA, PS-DETA, and PS-TETA. This implies that the three resins can be successfully applied for the recovery of Hg(II) from water and wastewater.

4. Conclusion

Three macroporous polystyrene-co-divinylbenzene-supported polyamine chelating resins (PS-EDA, PS-DETA, and PS-TETA) for use in the selective adsorption of to toxic Hg(II) ions is described. The following results were obtained:

(1) The polyamine-functional chelating resins had a remarkable selectivity for Hg(II) ions. The adsorption capacity for Hg(II) ions on PS-EDA, PS-DETA, and PS-TETA was (1.55, 1.73, and 1.84) mmol·g^{-1}, respectively.

(2) Kinetic studies on adsorption of Hg(II) ions on PS-EDA, PS-DETA, and PS-TETA revealed that pseudo-second-order model showed the best fit to the experimental data and that film diffusion might be involved in the adsorption process. Further, the adsorption activation energy, E_a, was equal to (6.24, 6.08, and 4.26) kJ·mol^{-1} for PS-EDA, PS-DETA, and PS-TETA,

which implied that Hg(II) ions were mainly adsorbed physically onto the chelating resins.

(3) The thermodynamic parameters $\Delta H°$, $\Delta G°$, and $\Delta S°$ of Hg(II) ion adsorption on PS-EDA, PS-DETA, and PS-TETA show endothermic heat of adsorption favored at high temperatures. The negative $\Delta G°$ values were indicative of the spontaneity of the adsorption process. The positive value of $\Delta S°$ showed an increase in randomness at the solid/solution interface during the adsorption of Hg(II) ions.

(4) The study of adsorption isotherms revealed that the Freundlich isotherm model gave the best fit to the experimental data.

(5) PS-EDA, PS-DETA, and PS-TETA chelating resins can selectively adsorb Hg(II) ions from binary ion systems in the presence of the coexistent ions Ni(II), Pb(II), Co(II), Cu(II), Zn(II), and Ag(I).

(6) The desorption rates of Hg(II)-loaded resins observed were 100 % for PS-EDA, PS-DETA, and PS-TETA.

Thus, it may be concluded that PS-EDA, PS-DETA, and PS-TETA chelating resins exhibited the potential for application in treatment of aqueous solutions containing Hg(II) ions. However, further research is needed to establish the process with specific attention to the regeneration of the chelating resins.

Literature Cited

(1) Francois, M. M. M; Anne, M. L. K; Marc, A. The chemical cycle and bioaccumulation of mercury. *Annu. Rev. Ecol. Syst.* **1998**, *29*, 543–566.

(2) Bailey, S. E.; Olin, T. J.; Bricka, R. M.; Adrian, D. D. A review of potentially low-cost sorbents for heavy metals. *Water Res.* **1999**, *33*, 2469–2479.

(3) Puanngam, M.; Unob, F. Preparation and use of chemically modified MCM-41 and silica gel as selective adsorbents for Hg(II) ions. *J. Hazard. Mater.* **2008**, *154*, 578–587.

(4) Starvin, A. M.; Rao, T. P. Removal and recovery of mercury(II) from hazardouswastes using 1-(2-thiazolylazo)-2-naphthol functionalized activated carbon as solid phase extractant. *J. Hazard. Mater.* **2004**, *113*, 75–79.

(5) Zhang, F. S.; Nriagu, J. O.; Itoh, H. Mercury removal from water using activated carbons derived from organic sewage sludge. *Water Res.* **2005**, *39*, 389–395.

(6) Atia, A. A.; Donia, A. M.; Elwakeel, K. Z. Selective separation of mercury(II) using a synthetic resin containing amine and mercaptan as chelating groups. *React. Funct. Polym.* **2005**, *65*, 267–275.

(7) Sun, C. M.; Qu, R. J.; Ji, C.N.; Wang, Q.; Wang, C. H.; Sun, Y. Z; Cheng, G. X. A chelating resin containing S, N and O atoms: synthesis and adsorption properties for Hg(II). *Eur. Polym. J.* **2006**, *42*, 188–194.

(8) Yavuz, E.; Senkal, B. F.; Bicak, N. Poly(acrylamide) grafts on spherical polyvinyl pyridine resin for removal of mercury from aqueous solutions. *React. Funct. Polym.* **2005**, *65*, 121–125.

(9) Merrifield, J. D.; Davids, W. G.; MacRae, J. D.; Amirbahman, A. Uptake of mercury by thiol-grafted chitosan gel beads. *Water Res.* **2004**, *38*, 3132–3138.

(10) Tonle, I. K.; Ngameni, E.; Njopwouo, D.; Carteret, C.; Walcarius, A. Functionalization of natural smectite-type clays by grafting with organosilanes: physico-chemical characterization and application to mercury(II) uptake. *Phys. Chem. Chem. Phys.* **2003**, *5*, 4951–4961.

(11) Walcarius, A.; Delacôte, C. Mercury(II) binding to thiol-functionalized mesoporous silicas: critical effect of pH and sorbent properties on capacity and selectivity. *Anal. Chim. Acta* **2005**, *547*, 3–13.

(12) Navarro, R. R.; Sump, K.; Fujii, N.; Matsumura, M. Mesury removal from wastewater using porous cellulose carrier modified with polyethyleneimine. *Water Res.* **1996**, *30*, 2488–2494.

(13) El-Nahhal, I. M.; El-Ashgar, N. M.; Chehimi, M. M.; Bargiela, P.; Maquet, J.; Babonneau, F.; Livage, J. Metal uptake by porous iminobis(N-2-aminoethylacetamide)-modified polysiloxane ligand system. *Microporous Mesoporous Mater.* **2003**, *65*, 299–310.

(14) Baba, Y.; Ohe, K.; Kawasaki, Y.; Kolev, S. D. Adsorption of mercury(II) from hydrochloric acid solutions on glycidylmethacrylate-divinylbenzene microspheres containing amino groups. *React. Funct. Polym.* **2006**, *66*, 1158–1164.

(15) Denizli, A.; Senel, S.; Alsancak, G.; Tüzmen, N.; Say, R. Mercury removal from synthetic solutions using poly(2-hydroxyethylmethacrylate) gel beads modified with poly(ethyleneimine). *React. Funct. Polym.* **2003**, *55*, 121–130.

(16) Groudeva, V. I.; Groudev., S. N.; Perkova, S. Biological treatment of acid drainage waters from a copper mine. *Miner. Slovaca* **1996**, *28*, 318–320.

(17) Sun, C. M.; Tang, Q. H.; Qu, R. J.; Ji, C. N.; Wang, C. H.; Cheng, G. X. Pore properties of crosslinked polystyrene supported polydiethanolamine-typed 'dendrimer-like' hyperbranched molecules. *Ion Exch. Adsorp.* **2007**, *23*, 307–313.

(18) Ji, C. N.; Qu, R. J.; Sun, C. M.; Wang, C. H.; Xu, Q.; Sun, Y. Z.; Li, C. X.; Guo, S. H. Macroporous Chelating Resins Incorporating Heterocyclic Functional Groups via Hydrophilic PEG Spacer Arms. I. Synthesis and Characterization. *J. Appl. Polym. Sci.* **2007**, *103*, 3220–3227.

(19) Barkat, M.; Nibou, D.; Chegrouche, S.; Mellah, A. Kinetics and thermodynamics studies of chromium(VI) ions adsorption onto activated carbon from aqueous solutions. *Chem. Eng. Process.* **2009**, *48*, 38–47.

(20) Ho, Y. S.; McKay, G.; Wase, D. A. J.; Foster, C. F. Study of the sorption of divalent metal ions on to peat. *Adsorp. Sci. Technol.* **2000**, *18*, 639–650.

(21) Ho, Y. S. Second-order kinetic model for the sorption of cadmium onto tree fern: a comparison of linear and non-linear methods. *Water Res.* **2006**, *40*, 119–125.

(22) Azizian, S. Kinetic models of sorption: a theoretical analysis. *J. Colloid Interface Sci.* **2004**, *276*, 47–52.

(23) Boyd, G. E.; Adamson, A. W.; Myers, L. S. The exchange adsorption of ions from aqueous solutions by organic zeolites. *J. Am. Chem. Soc.* **1947**, *69*, 2836–2848.

(24) Reichenberg, D. Properties of ion-exchange resins in relation to their structure. III. kinetics of exchange. *J. Am. Chem. Soc.* **1953**, *75*, 589–592.

(25) Khambhaty, Y.; Mody, K.; Basha, S.; Jha, B. Kinetics, equilibrium and thermodynamic studies on biosorption of hexavalent chromium by dead fungal biomass of marine Aspergillus niger. *Chem. Eng. J.* **2009**, *145*, 489–495.

(26) Rao, R. A. K.; Khan, M. A. Biosorption of bivalent metal ions from aqueous solution by an agricultural waste: Kinetics, thermodynamics and environmental effects. *Colloids Surf., A* **2009**, *332*, 121–128.

(27) Nollet, H.; Roels, M.; Lutgen, P.; Van der Meeren, P.; Verstrate, W. Removal of PCBs from wastewater using fly ash. *Chemosphere* **2003**, *53*, 655–665.

(28) Zhu, J.; Deng, B.; Yang, J.; Gang, D. Modifying activated carbon with hybrid ligands for enhancing aqueous mercury removal. *Carbon* **2009**, *47*, 2014–2025.

(29) Barkat, M.; Nibou, D.; Chegrouche, S.; Mellah, A. The positive value of $\Delta S°$ reflects the affinity of Hg(II) for the resins used. Kinetics and thermodynamics studies of chromium(VI) ions adsorption onto activated carbon from aqueous solutions. *Chem. Eng. Process.* **2009**, *48*, 38–47.

(30) Khambhaty, Y.; Mody, K.; Basha, S.; Jha, B. Kinetics, equilibrium and thermodynamic studies on biosorption of hexavalent chromium by dead fungal biomass of marine Aspergillus niger. *Chem. Eng. J.* **2009**, *145*, 489–495.

(31) Ramesh, A.; Hasegawa, H.; Sugimoto, W.; Maki, T.; Ueda, K. Adsorption of gold(III), platinum(IV) and palladium(II) onto glycine modified crosslinked chitosan resin. *Bioresour. Technol.* **2008**, *99*, 3801–3809.

(32) Karadag, D.; Turan, M.; Akgul, E.; Tok, S.; Faki, A. Adsorption equilibrium and kinetics of reactive black 5 and reactive red 239 in aqueous solution onto surfactant-modified zeolite. *J. Chem. Eng. Data* **2007**, *52*, 1615–1620.

(33) Febrianto, J.; Kosasiha, A. N.; Sunarso, J.; Ju, Y. H.; Indraswati, N.; Ismadji, S. Equilibrium and kinetic studies in adsorption of heavy metals using biosorbent: A summary of recent studies. *J. Hazard. Mater.* **2009**, *162*, 616–645.

(34) Volesky, B. *Biosorption of heavy metals*; CRC Press: Boca Raton, FL, 1990.

(35) Jeon, C.; HÖll, W. H. Chemical modification of chitosan and equilibrium study for mercury ion removal. *Water Res.* **2003**, *37*, 4770–4780.

Received for review March 17, 2010. Accepted August 28, 2010. The authors are grateful for the financial support by the National Natural Science Foundation of China (Grant No. 51073075), Natural Science Foundation of Shandong Province (No. ZR2009FM075, 2008BS04011, Y2007B19), the Nature Science Foundation of Ludong University (No. 08-CXA001, 032912, 042920, LY20072902), and Educational Project for Postgraduate of Ludong University (No. YD05001, Ycx0612).

JE100246Y